Visible and near IR emitting organic nanoparticles of aromatic fumaronitrile core-based donor–acceptor compounds

Krishna Panthi [a], Ravi M. Adhikari [b], Thomas H. Kinstle [a,*]

[a] Department of Chemistry, Center for Photochemical Sciences, Bowling Green State University, Bowling Green, OH 43403, United States
[b] Angstrom Technologies Incs, Florence, KY 41042, United States

ABSTRACT

A class of five compounds (**1–5**) having aromatic fumaronitrile as electron acceptor, phenylacetylene as linker and carbazole, indole, or diphenylamine moieties as electron donors, has successfully formed fluorescent organic nanoparticles (FONs) in THF/water mixtures. FONs formed from these compounds emit from the visible region to the near IR region. The fluorescence intensity of compound **1** is increased by 19 times upon the formation of nanoparticles compared to its THF solution. A large Stokes shift of 256 nm has been observed during the formation of nanoparticles of compound **4**. The potential application of these FONs in dye sensitized solar cells, optoelectronic device fabrication, and biomedical imaging is under assessment.

© 2010 Elsevier B.V. All rights reserved.

1. Introduction

In the recent past, several fluorescent inorganic and composite nanoparticles have been prepared and investigated for various applications such as in light emitting devices [1,2], in photovoltaics [3], as biological nanosensors [4], and the drug delivery technologies [5]. For these applications, major efforts to generate inorganic semiconductors and metal nanoparticles have been made with considerable success, but relatively few approaches have been reported to organic nanostructures [6]. Recently, several articles report that fluorescent organic nanoparticles (FONs) show size dependent absorption and emission characteristics [7,8]. Systematic research on FONs has been initiated by Nakanishi and coworkers [9–11]. Upon formation of nanoparticles, arylethynyl compound [12], pentaphenylsilole [13], and 1-cyano-trans-1,2-bis-(4′-methylbiphenyl)ethylene [7] give enhanced fluorescence, compared to the generally observed fluorescence quenching in the solid state [14]. The emission enhancement in nanoparticles is probably because of the effects of intramolecular planarization and a specific intermolecular aggregation in the solid state.

There is considerable interest in the development of materials and devices that exhibit wavelength tunability and efficient light emission in the near IR (NIR) wavelength region [15]. The first report of NIR emission from an organic light-emitting device (OLED) based on a lanthanide complex [16] has lead to the pursuit of applications in the defense, telecommunication, and biomedical imaging fields [17]. Light emitting nano-materials, if properly emissive, could provide a source of white light at a greatly reduced cost for application in full color electronic displays. Organic NIR emitting particles have the advantage of low cost, flexible synthesis and lowered toxicity and their availability should stimulate new applications in various fields. In this article we have reported the first preparation of NIR emitting FONs and studied their optical properties to assess their potential applications. We herein report two different sub-classes of compounds that form FONs-one class of compounds that retains optical purity upon the formation of FONs accompanied by increased fluorescence intensity and the other class of compounds that show a large red shift of emission into the near IR but diminished fluorescence intensity upon the formation of FONs. We have chosen to study electron donor acceptor compounds containing an aromatic fumaronitrile core because fumaronitrile core based compounds have shown useful emission properties in electroluminescent (EL) devices [18,19]. Palayangoda et at. [20] have reported aromatic fumaronitrile core based carbazole compounds form fluorescent nanoparticles. We have reported [21] the synthesis and photophysics of the aromatic fumaronitrile core based electron donor–acceptor compounds 2,3-bis(4-(1H-indol-1-yl)phenyl)fumaronitrile (**1**), 2,3-bis(4-(2-phenyl-1H-indol-1-yl)phenyl)fumaronitrile (**2**), 2,3-bis(4-(diphenylamino)phenyl)fumaronitrile (**3**), 2,3-bis(4-

* Corresponding author. Tel.: +1 419 575 2064.
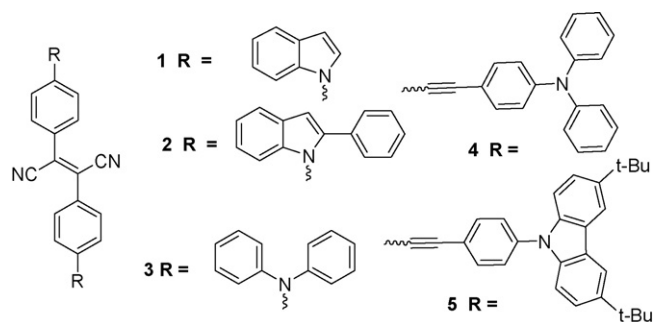 *E-mail address:* tkinstl@bgsu.edu (T.H. Kinstle).

Fig. 1. Structures of compounds **1**–**5**.

Fig. 2. Absorption spectra of **1** nanoparticles solution (1×10^{-5} M) recorded at different THF and THF/H_2O mixtures.

(2-(4-(diphenylamino)phenyl)ethynyl)phenyl)fumaronitrile (**4**), and 2,3-bis(4-(2-(4-(3,6-di-tert-butyl-9H-carbazol-9-yl)phenyl)-ethynyl) phenyl)fumaronitrile (**5**). Here we report the formation and properties of fluorescent nanoparticles formed from these compounds **1**–**5** (Fig. 1).

Nanoparticles of compounds **1**–**5** were prepared by a simple reprecipitation technique [20,22]. Identical concentrations of solutions (1×10^{-5} M) were prepared for all THF/water mixtures (1:4, 1:8, 1:12, and 1:16). The suspension of nanoparticles formed was visibly transparent and stable at ambient temperature. Spectral properties of all samples were unchanged after three months.

2. Experimental

2.1. Fluorescence lifetime (τ) measurement

The compounds in THF and THF/water mixtures were put in quartz cuvettes. Fluorescence decay profiles of the argon-degassed samples were measured using a single photon counting spectrofluorimeter. The model of the spectrofluorimeter is HORIBA Jobin Yvon Fluorolog FL3-11. The resolution of the instrument is nanosecond and the excitation source is nano-LED. Decays were monitored at the corresponding emission maximum of the samples. In-built software allowed the fitting of the decay spectra ($\chi = 1$–1.5) and produced the fluorescence lifetimes.

2.2. Preparation of nanoparticles

Samples of predetermined concentrations of **1**–**5** in THF were made. The appropriate volumes of these solutions were placed in different vials and the required amount of water was rapidly injected into those vials while maintaining the final concentrations of the solutions the same. Four different THF/water ratios i.e., 1:4, 1:8, 1:12, and 1:16 for each compound were made. In all samples the formation of nanoparticles could be observed by irradiation using 365 nm UV lamp. In some samples formation of nanoparticles could be seen by the naked eye because of change of color of the transparent solution.

2.3. SEM images of nanoparticles

Scanning electron microscopy (SEM) images were recorded on a FEI-FP2031/11 microscope at 15 eV using INCA Penta FETX3 detector. Samples for SEM were prepared by placing few drops of nanoparticle suspension onto a glass cover slip placed on an aluminum stub. The samples were allowed to dry at room temperature before observing under the scanning electron microscope. To enhance the contrast and quality of the SEM images, the samples were sputter-coated with gold/palladium.
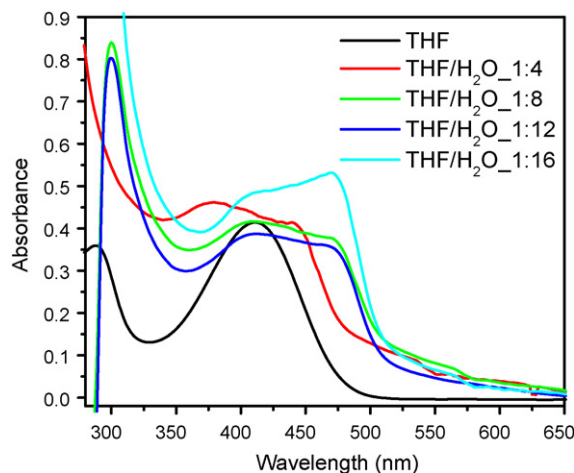
2.4. Fluorescent microscopy (FM) images of nanoparticles

Fluorescent microscopy images were recorded on a Qimaging Epi Fluorescence Microscope using QICAM camera. The data were collected using Metaphor software in computer. The samples were prepared by putting a droplet of nanoparticles suspension on a glass slide and covering with a cover slip.

2.5. Confocal microscopy images of the nanoparticles

Confocal microscopy images were obtained using an Olympus FluoView 1000 microscope. The same method employed to prepare the samples for FM images was used to prepare the samples for confocal microscopy images.

The excitation source was a diode blue laser (405 nm), and fluorescence was detected using standard three confocal channels (three photomultiplier detectors). The emission filter (BA535-565) at 405 nm laser light for green emission and the emission filter (BA 650 IF) at 488 nm laser light were used for the image recording.

3. Results and discussion

3.1. UV–vis spectra and nanoparticles of compounds **1**–**3**

UV–vis spectra of **1** in THF and as nanoparticles suspended in solvents differing in the THF/water ratio are displayed in Fig. 2. Compound **1** shows two distinct peaks about 300 nm and about 410 nm in THF. With the addition of water the absorption transition associated with the indole moiety (about 300 nm) slightly red shifts. This may be due to the electronic coupling between the neighboring molecules as they approach each other in THF/water mixture because of the hydrophobic nature of **1**. 1,3-Diphenyl-5-(2-anthryl)-2-pyrazoline-based nanoparticles exhibit a similar behavior [23]. The peak around 410 nm, which can be assigned to the transition from S_o to intramolecular charge transfer (ICT) state, shifted to red. As the ratio of water is further increased, a new absorption band around (470 nm) appears. This is assigned to a transition from S_o to an ICT state [24] that forms as the molecules of **1** are assembled even more closely and begin nucleating into nanoparticles. The comparative intensity around 470 nm increases with the fraction of water. It is likely that intramolecular interaction originates from overlapping of the indole moiety and the nitrile group of the neighboring molecules vide infra, which further increases as the nucleation progresses [25–28]. The molecular overlap is also strengthened by an increase in the molecular dipole
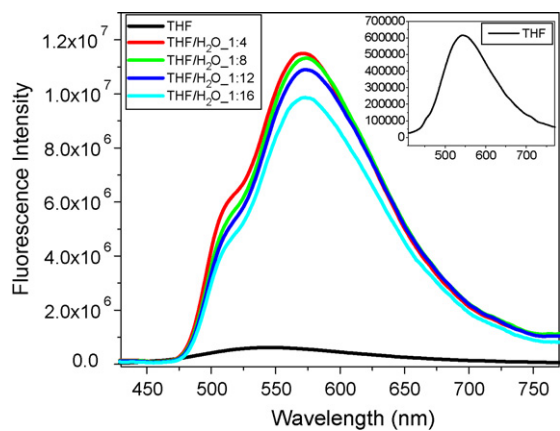
Fig. 3. Emission spectra of **1** nanoparticles solution (1×10^{-5} M) recorded at different THF and THF/H_2O mixtures. Sample solutions were excited at 440 nm. (inset: the enlarged spectrum of **1** recorded in THF).

Fig. 4. Absorption spectra of **4** nanoparticles solution (1×10^{-5} M) recorded at different THF and THF/H_2O mixtures.

and the ICT state becomes more prominent. These results in the red-shifted absorption vide infra [23,24,29]. Additionally; Mie scattering may also be responsible for the red shift in the absorption transition [7].

There are significant differences between the fluorescence spectrum of **1** in THF and the spectra of **1** nanoparticles formed in the THF/water medium (Fig. 3). The emission of **1** in THF around 550 nm is due to the radiative deactivation of ICT excited state to ground state. On increasing the fraction of water the emission intensity is enhanced and is accompanied with a slight red shift. The ICT state of the **1** nanoparticles is responsible for the broad emission (500 nm to 700 nm) that appears at the higher water ratio. It is likely that an n-electron from nitrogen of the indole moiety transfers to the nitrile moiety of the same molecule, resulting in the ICT state. This leads to an increase in the dipole moment of **1** in the nanoparticle state, which in turn enhances the intermolecular interaction. A similar charge transfer phenomenon was observed in 1-phenyl-3-((dimethylamino)styryl)-5-((dimethylamino)phenyl)-2-pyrazoline-based nanoparticles [6]. The size of nanoparticles increases with an increase in the fraction of water [8]. This allows the intermolecular electronic interactions to extend over a large number of molecules and to increase in magnitude. This is likely the reason for the significantly red-shifted emission of the **1** nanoparticles compared to that from the individual molecules of compound **1**. A red-shifted emission is expected for an aggregate state [21,23,30,31] arising from the extended orbital overlap of closely stacked molecules in nanoparticles [18]. According to the molecular exciton model, head-to-tail alignment of transition dipole (J aggregation) shifts emission to the red region and enhances fluorescences. The main reason for an enhanced emission in J aggregation is the planarization of the molecule in nanoparticles [24]. Similar results were observed for compound **3** in THF and as nanoparticle suspensions. Compounds **1** and **3** have the same linker and are planar.

The red-shifted absorption of **1** and **3** in THF/water ratios indicate J-type of aggregation. Compound **2** does not show any effect on continued addition of water to the THF solution other than slight intensity change in absorption and emission. It does not have a sufficiently strong electron donor (ED) to form ICT. In compounds **1** and **3**, the emission intensity of nanoparticles in suspension is stronger than that in THF (Fig. 3 and Supporting Information). It has been observed that for compound **1** the intensity of emission for nanoparticles has increased by 19 times but in compound **3** the intensity has increased only by 9 fold. We were able to maintain the color purity with an increase in fluorescence intensity in compounds **1** and **3** upon formation of nanoparticles. For compound **2**
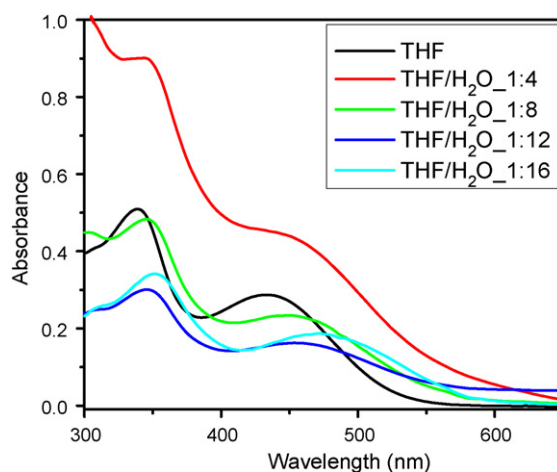
there is no significant change in intensity and red shift of absorption and emission during the formation of nanoparticles.

3.2. UV–vis spectra and nanoparticles of compounds **4** and **5**

For compounds **4** and **5**, significant red shift of absorption and emission has been observed for nanoparticles compared to their THF solutions (Figs. 4 and 5, Table 1 and Supporting Information). In THF solution **4** forms ICT and **5** forms TICT both in ground state and excited state as THF stabilizes the CT [21]. But when they form nanoparticles on addition of water they are pushed out of solvent cage. Compound **4** forms ICT in nanoparticle form as it is more planar but compound **5**, a non-planar structure [21], and forms intermolecular charge transfer state. Both **4** and **5** show diminished emission intensity as nanoparticles in THF/water suspension compared to that of THF solution. The main reason for an enhanced emission in J aggregation is the planarization of the molecule in nanoparticles. It is likely that the **4** and **5** molecules undergo J aggregation facilitating inter- or intramolecular charge transfer, but retains the non-planar or twisted structure.

Nanoparticle suspensions of **4** emit in the near IR region with a huge Stokes shift. This is the first time to our knowledge where NIR emission from organic nanoparticles has been reported. Since compound **4** is planar, intramolecular electron transfer from electron donor to electron acceptor is significant even in the nanoparticle forms. Again in the nanoparticle form intermolecular electronic
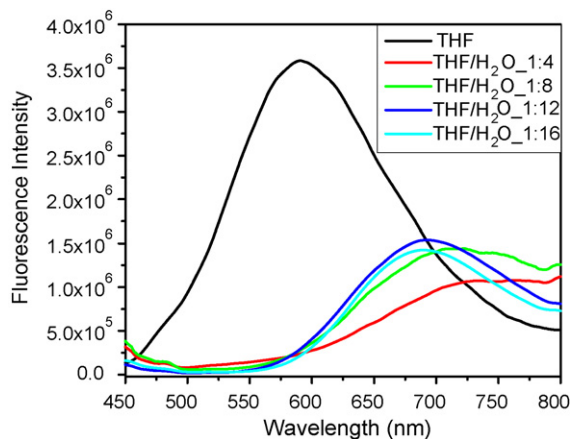

Fig. 5. Emission spectra of **4** nanoparticles solution (1×10^{-5} M) recorded at different THF and THF/H_2O mixtures. Sample solutions were excited at 440 nm.

Table 1
Absorption maximum (A_{max}), emission maximum (λ_{max})[a], molar extinction coefficient (ε), red shift of emission, and lifetime (τ) of compounds **1–5** in THF and THF/H$_2$O mixtures.

Compound	Ratio of solvents	A_{max} (nm)	ε (M^{-1} cm^{-1})	λ_{max} (nm)	Red shift (nm) (emission)	Lifetime (τ) (ns)
	THF/Water_1:0	410	23174	542	–	2.97
	THF/Water_1:4	387–472	16222	572	30	3.26
1	THF/Water_1:8	400–470	14167	572	30	5.34
	THF/Water_1:12	400–470	10741	572	30	4.83
	THF/Water_1:16	400–470	9127	572	30	4.69
	THF/Water_1:0	306	45734	359	–	1.33
	THF/Water_1:4	306	87118	363	4	0.18
2	THF/Water_1:8	306	66363	363	4	0.02
	THF/Water_1:12	306	51371	363	4	0.16
	THF/Water_1:16	306	33720	363	4	0.05
	THF/Water_1:0	471	20749	644	–	0.34
	THF/Water_1:4	490	30188	644	0	1.36
3	THF/Water_1:8	490	25254	644	0	1.81
	THF/Water_1:12	490	26008	644	0	1.73
	THF/Water_1:16	490	26145	644	0	1.76
	THF/Water_1:0	436	49357	490	–	5.19
	THF/Water_1:4	442	60337	746	256	1.04
4	THF/Water_1:8	450	53651	716	236	9.7
	THF/Water_1:12	457	29034	693	203	12.69
	THF/Water_1:16	470	39764	692	202	14.31
	THF/Water_1:0	345	43749	418	–	1.99
	THF/Water_1:4	345	53560	524	106	3.22
5	THF/Water_1:8	345	47687	620	202	3.75
	THF/Water_1:12	345	40313	609	191	2.85
	THF/Water_1:16	345	37956	605	186	1.81

[a] Emissions are measured by exciting at the absorption maximum of each compound.

interactions extends over a large number of molecules and also increases in magnitude arising from the extended orbital overlap of closely stacked molecules in nanoparticles.

It has been observed that for compound **4** the emission for nanoparticles has been red shifted by 256 nm (Fig. 5). In compounds **4** the formation of nanoparticles can be seen by the naked eye as a noticeable change of color due to the large red shift of absorption and emission. Thus, in compounds **4** and **5**, with the formation of nanoparticles, the tuning of emission toward the near IR region from visible region was achieved.

Interestingly, the absorption spectra of compound **4** are more blue shifted in all solvents compared to the absorptions of compound **3**, even though the former compound has one more phenylethynyl moiety to increase conjugation length. Likewise, the emission maxima of compound **4** are also at higher energies than that of compound **3**. The two additional phenylethynyl moieties in **4** increase its rotational flexibility so that the electrons from the nitro-gen atom of the diphenylamine group cannot be easily transported towards the cyano group. In nanoparticles of **3** and **4**, the emission of **4** is red shifted (up to 256 nm) but in compound **3** there is no red shift in emission of nanoparticles but the intensity has increased 9 fold. Similar results were observed for compound **5** having two more phenylethynyl moieties than the 1,2-dicyano-trans-1,2-bis-4(3,6-di-tert-butylcarbazolyl)phenylethylene compound that Palayangoda et al. [20] reported.

3.3. Size and lifetime of nanoparticles of compounds **1–5**

The size of the nanoparticles was determined using scanning electron microscopy (SEM) (Fig. 6 and Supporting Information) and the particle sizes are about 233 nm, 210 nm, 630 nm, 650 nm and 203 nm for compounds **1–5**, respectively. There is no remarkable change in absorption, emission or particle size with the higher fractions of water in THF. For all compounds, we obtained the best
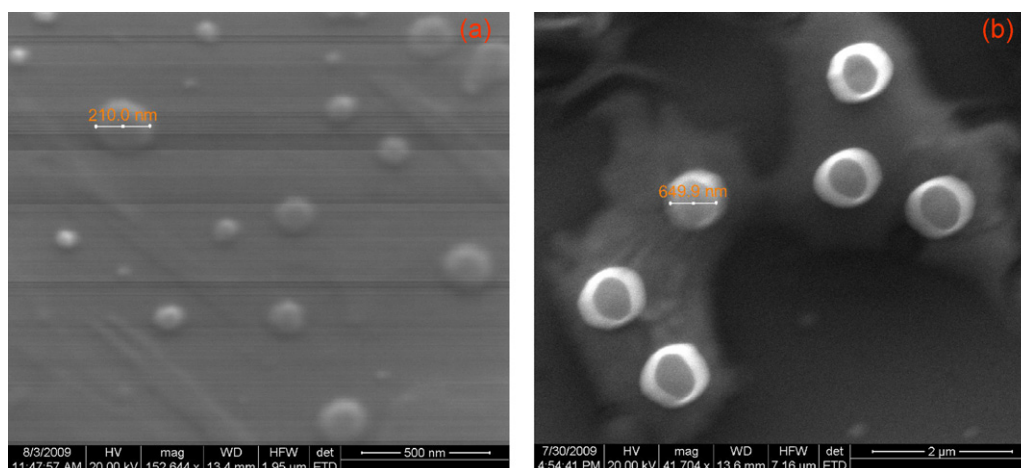

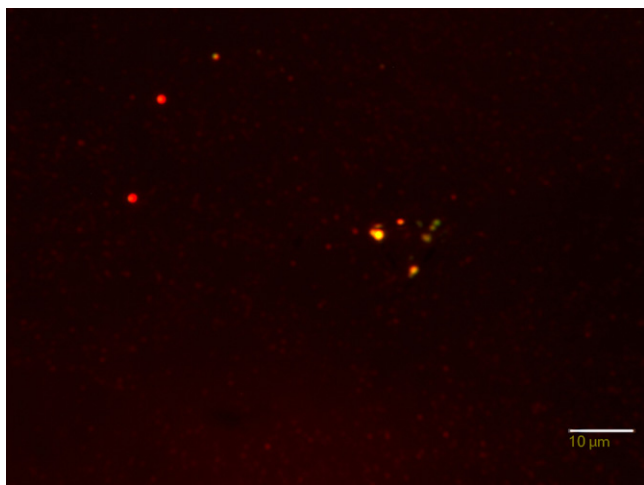**Fig. 6.** SEM images of nanoparticles of compound **2** (a) and **4** (b) in THF/H$_2$O_1:8.

Fig. 7. Fluorescent Microscopy (FM) image of nanoparticles of compound **4** in THF/H$_2$O 1:8.

Fig. 9. Solutions of compound **1** from left to right in THF and THF/H$_2$O mixtures in the ratio of 1:0, 1:4, 1:8, 1:12, and 1:16. The concentrations of all solutions were 1×10^{-5} M.

Fig. 10. Solutions of compound **4** from left to right in THF and THF/H$_2$O mixtures in the ratio of 1:0, 1:4, 1:8, 1:12, and 1:16. The concentrations of all solutions were 1×10^{-5} M.

nanoparticles in terms of emission intensity and in terms of red shift in a 1:4 THF/water solution, but we obtained SEM images for nanoparticles obtained in 1:8 THF/water since the size of nanoparticles in the more THF rich solutions might have been too small to take images [8]. We also scanned the fluorescent microscopy (FM) images of nanoparticles for all compounds for THF/water 1:8 mixture to judge how fluorescent these nanoparticles were (Fig. 7, and Supporting Information). The size distribution of nanoparticles from all compounds was rather large. As shown by some literatures [8], we did not find the direct correlation between the fractions of water with the red shift of emission, though with higher fractions of water we observe red shift on emission. But there are some reports which do not show the same correlation is true [20].

The emission properties of all compounds were further investigated using a confocal microscope (Fig. 8 and Supporting Information). Green light emission was observed from the nanoparticles of compounds **1** and **3**, and red light emission was observed from the nanoparticles of compound **4**. This assured us that the red emission is indeed from the nanoparticles since there is no solvent to interfere the emission. These FONs were stable to a blue laser for hours.
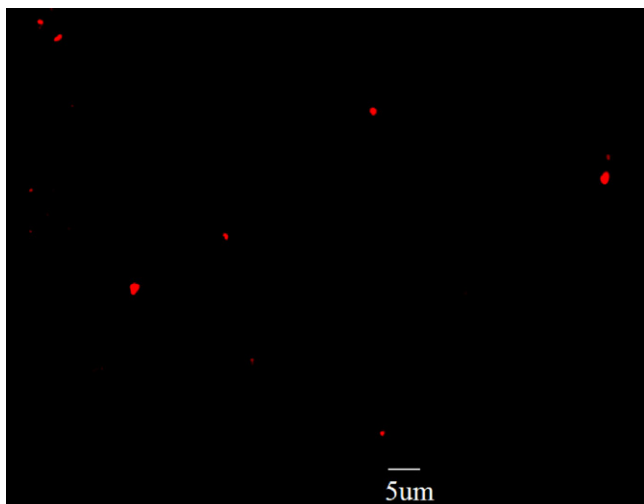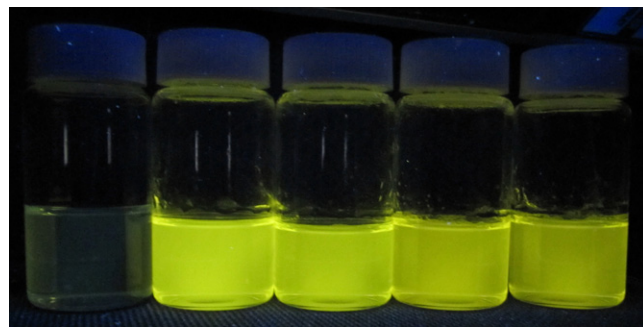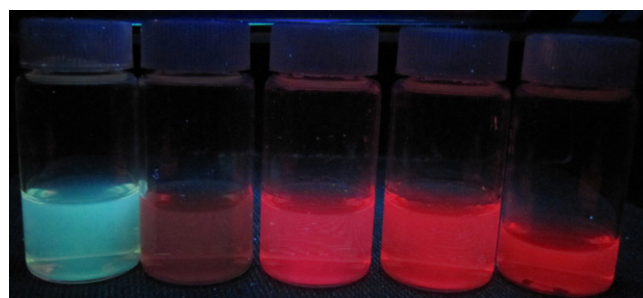
The formation of nanoparticles is clearly associated with the addition of water. Water and THF are miscible, so the solubility of hydrophobic compounds decreases with the increasing fraction of water, eventually reaching a critical nucleation condition at which nuclei form throughout the solution and begin to grow as particles [32]. Once the concentration of solute in solution falls due to the growing nuclei, particle growth stops so that the equilibrium mixture contains both particles and solution.

We further measured the fluorescence lifetimes ($_F$) of compounds in dilute THF solutions and as nanoparticles dispersed in different fractions of THF/water (Table 1). The excitation source used was nano-LED and was excited using 350 nm nano-LED for compound **2** and **3**, and 560 nm for compounds **1**, **4**, and **5**. Decays were monitored at the corresponding emission maxima (λ_{max}). All compounds follow monoexponential decay. Usually the lifetimes of fluorescence are higher for samples with higher fraction of water with some exceptions. The same result has been observed by authors [8].

The emission of nanoparticles of compound **4** could be reversibly shifted yellow or NIR, through an adjustment in the THF/water ratio. The fluorescence maximum of **4** nanoparticles (Fig. 5), for example, shifted from 410 to 590 nm with an increase in water. In contrast, increasing the THF ratio with such samples caused the fluorescence emission to revert to its initial value (410 nm) (Supporting Information). Changes in emission color of compounds **1** and **4** in THF and THF water mixtures on excitation at 365 nm is illustrated in Figs. 9 and 10, respectively.

4. Conclusions

The FONs were prepared from five different compounds and their optical properties were measured using absorption spectroscopy, fluorescence spectroscopy, scanning electron microscopy, fluorescence microscopy and confocal microscopy. Their optical properties were further assessed by the measure-

Fig. 8. Confocal Microscopy image of nanoparticles of compound **4** in THF/H$_2$O 1:8.

ment of lifetimes of fluorescence at various ratios of THF/water maintaining the same concentration. In some compounds we were able to retain the optical purity upon the formation of FONs. Compounds **4** and **5** showed tunable emission properties upon formation of nanoparticles. This is the first example that NIR emission was achievable upon the formation of nanoparticles from pure organic compounds. The potential application of this property is under active investigation. Stokes shift of as much as 256 nm was achieved using compound **4**. Emission was enhanced by as much as 19 times in compound **1** upon the formation of nanoparticles. Reversible switching of emission with a change in THF/water ratio was illustrated. A possible alignment of molecules that is responsible for the high Stokes shift in nanoparticles was discussed.

Acknowledgements

Appendix A. Supplementary data

Suppplementary data associated with this article (UV-visible spectra of suspensions of compounds in THF and THF/H2O mixtures (THF/H2O ratio 1:0, 1:4, 1:8, 1:12, and 1:16), SEM images, FM images, and Confocal Microscopy images of nanoparticles. Supporting Information also includes solution of compounds in THF and THF/water mixtures under UV light) can be found, in the online version, at doi:10.1016/j.jphotochem.2010.08.014.

References

[1] M.C. Schlamp, X. Peng, A.P. Alivisatos, Improved efficiencies in light emitting diodes made with CdSe (CdS) core/shell type nanocrystals and a semi conducting polymer, J. Appl. Phys. 82 (1997) 5837–5842.
[2] D.Y. Godovsky, Devices applications of polymer-nanocomposites, Adv. Polym. Sci. 153 (2000) 163–205.
[3] M. Grätzel, Mesoporous oxide junctions and nanostructured solar cells, Curr. Opin. Colloid Interface Sci. 4 (1999) 314–321.
[4] A.N. Shipway, E. Katz, I. Willner, Nanoparticle arrays on surface for electronic, optical and sensors applications, ChemPhysChem 1 (2000) 18–52.
[5] M. El-Kemary, H. Yao, Synthesis, characterization and optical properties of organic nanoparticles of piroxicam anti-inflammatory drug, Photochem. Photobiol. A: Chem. 212 (2010) 170–175.
[6] H.-B. Fu, J.-N. Yao, Size effects on the optical properties of organic nanoparticles, J. Am. Chem. Soc. 123 (2001) 1434–1439.
[7] B.-K. An, S.-K. Kwon, S.-D. Jung, S.Y. Park, Enhanced emission and its switching in fluorescent organic nanoparticles, J. Am. Chem. Soc. 124 (2002) 14410–14415.
[8] R.M. Adhikari, B.K. Shah, S.S. Palayangoda, D.C. Neckers, Solvent dependent optical switching in carbazole-based fluorescent nanoparticles, Langmuir 25 (2009) 2402–2406.
[9] H. Kasai, Y. Yoshikawa, T. Seko, S. Okada, H. Oikawa, H. Matsuda, A. Watanabe, O. Ito, H. Toyotama, H. Nakanishi, Optical properties of perylene microcrystals, Mol. Cryst. Liq. Cryst. 294 (1997) 173–176.

[10] H. Kasai, H. Kamatani, S. Okada, H. Oikawa, H. Matsuda, H. Nakanishi, Size-dependent colors and luminescences of organic microcrystals, Jpn. J. Appl. Phys. 34 (1996) L221–L223.
[11] H. Kasai, H. Kamatani, Y. Yoshikawa, S. Okada, H. Oikawa, A. Watanabe, O. Ito, H. Nakanishi, Crystal size dependence of emission from perylene microcrystals, Chem. Lett. (1997) 1181–1182.
[12] M. Levitus, K. Schmieder, H. Ricks, K.D. Shimizu, U.H.F. Bunz, M.A. Garcia-Garibay, Steps to demarcate the effects of chromophore aggregation and planarization in poly(phenyleneethynylene)s. 1. Rotationally interrupted conjugation in the excited states of 1,4-bis(phenylethynyl)benzene, J. Am. Chem. Soc. 123 (2001) 4259–4265.
[13] J. Luo, Z. Xie, J.W.Y. Lam, L. Cheng, H. Chen, C. Qiu, H.S. Kwok, X. Zhan, Y. Liu, D. Zhu, B.Z. Tang, Aggregation-induced emission of 1-methyl-1,2,3,4,5-pentaphenylsilole, Chem. Commun. (2001) 1740–1741.
[14] J.B. Birks, Photophysics of Aromatic Molecules, Wiley, London, 1970.
[15] Y. Yang, R.T. Farley, T.T. Steckler, S.-H. Eom, J.R. Reynolds, K.S. Schanze, J. Xue, Near infrared organic light-emitting devices based on donor–acceptor–donor oligomers, Appl. Phys. Lett. 93 (2008) 163305-1–163305-3.
[16] R.G. Sun, Y.Z. Wang, Q.B. Zheng, H.J. Zhang, A.J. Epstein, 1.54 µm infrared photoluminescence and electroluminescence from an erbium organic compound, J. Appl. Phys. 87 (2000) 7589–7591.
[17] R.J. Curry, W.P. Gillin, 1.54 µm electroluminescence from erbium (III) tris(8-hydroxyquinoline) (ErQ)-based organic light emitting diodes, Appl. Phys. Lett. 75 (1999) 1380–1382.
[18] H.-C. Yeh, S.-J. Yeh, C.-T. Chen, Readily synthesized arylamino fumaronitrile for non-doped red organic light-emitting diodes, Chem. Commun. (2003) 2632–2633.
[19] Chen, C.-T. Chen, Evolution of red organic light-emitting diodes: materials and devices, Chem. Mater. 16 (2004) 4389–4400.
[20] S.S. Palayangoda, X. Cai, R.M. Adhikari, D.C. Neckers, Carbazole-based donor–acceptor compounds: highly fluoresent organic nanoparticles, Org. Lett. 10 (2008) 281–284.
[21] K. Panthi, R.M. Adhikari, T.H. Kinstle, Aromatic fumaronitrile core-based donor-linker–acceptor-linker–donor (d–π–a–π–d) compounds: synthesis and photophysical properties, J. Phys. Chem. A 114 (2010) 4542–4549.
[22] K. Panthi, R.M. Adhikari, T.H. Kinstle, Carbazole donor–carbazole linker-based compounds: preparation, photophysical properties and formation of fluorescent nanoparticles, J. Phys. Chem. A 114 (2010) 4550–4557.
[23] D. Xiao, L. Xi, W. Yang, H. Fu, Z. Shuai, F. Yan, J. Yao, Size-tunable emission from 1,3-diphenyl-5-(2-anthryl)-2-pyrazoline nanoparticles, J. Am. Chem. Soc. 125 (2003) 6740–6745.
[24] H. Fu, B.H. Loo, D. Xiao, R. Xie, X. Ji, J. Yao, B. Zhang, L. Zhang, Multiple emissions from 1,3-diphenyl-5-pyrenyl-2-pyrazoline nanoparticles: evolution from molecular to nanoscale to bulk materials, Angew. Chem. Int. Ed. 41 (2002) 962–965.
[25] A.P. Alivisatos, Semiconductor clusters, nanocrystals, and quantum dots, Science 271 (1996) 933–937.
[26] X.G. Peng, M.C. Schlamp, A.V. Kadavanich, A.P. Alivisatos, Epitaxial growth of highly luminescent cdse/cds core/shell nanocrystals with photostability and electron accessibility, J. Am. Chem. Soc. 119 (1997) 7019–7029.
[27] X.G. Peng, L. Manna, W.D. Yang, J. Wickham, E. Scher, A. Kadavanich, A.P. Alivisatos, Shape control of CdSe nanocrystals, Nature 404 (2000) 59–61.
[28] D. Oelkrug, A. Tompert, J. Gierschner, H.-J. Egelhaaf, M. Hanack, M. Hohloch, E. Steinhuber, Tuning of fluorescence in films and nanoparticles of oligophenylenevinylenes, J. Phys. Chem. B 102 (1998) 1902–1907.
[29] M. Bruchez, M. Moronne, P. Gin, S. Weiss, A.P. Alivisatos, Semiconductor nanocrystals as fluorescent biological labels, Science (1998) 2013–2016.
[30] M.-X. Yu, L.-C. Chang, C.-H. Lin, J.-P. Duan, F.-I. Wu, I.-C. Chen, C.-H. Cheng, Luminescence properties of benzathrones and their application as host emitters in organic light emitting devices, Adv. Funct. Mater. 17 (2007) 369–378.
[31] A.E. Nikolaev, G. Myszkiewicz, G. Berden, W.L. Meerts, J.F. Pfanstiel, D.W. Pratt, Twistel intramolecular charge transfer states: rotationally resolved fluorescence excitation spectra of 4,4′-dimethylaminobenzonitrile in a molecular beam, J. Chem. Phys. 122 (2005) 84309–84310.
[32] D. Horn, J. Rieger, Organic nanoparticles in the aqueous phase-theory, experiment and use, Angew. Chem. Int. Ed. 40 (2001) 4330–4361.